Reduction of Variance-related Error through Ensembling: Deep Double Descent and Out-of-Distribution Generalization

Pavlos Rath-Manakidis, Hlynur Davíð Hlynsson and Laurenz Wiskott
Institut für Neuroinformatik, Ruhr-Universität Bochum, Bochum, Germany

Keywords: Deep Double Descent, Ensemble Model, Error Decomposition.

Abstract: Prediction variance on unseen data harms the generalization performance of deep neural network classifiers. We assess the utility of forming ensembles of deep neural networks in the context of double descent (DD) on image classification tasks to mitigate the effects of model variance. To that end, we propose a method for using geometric-mean based ensembling as an approximate bias-variance decomposition of a training procedure's test error. In ensembling equivalent models we observe that ensemble formation is more beneficial the more the models are correlated with each other. Our results show that small models afford ensembles that outperform single large models while requiring considerably fewer parameters and computational steps. We offer an explanation for this phenomenon in terms of model-internal correlations. We also find that deep DD that depends on the existence of label noise can be mitigated by using ensembles of models subject to identical label noise almost as thoroughly as by ensembles of networks each trained subject to i.i.d. noise. In the context of data drift, we find that out-of-distribution performance of ensembles can be assessed by their in-distribution performance. This aids in ascertaining the utility of ensembling for generalization.

1 INTRODUCTION

In the field of deep learning the process of deriving models is normally subject to multiple internal and external sources of randomness and noise. Their influence is such that the realized predictors – even if their performance scores on the test set are almost equal – realize measurably different mappings. It is therefore beneficial to analyse such influences and try to reduce their adverse effects. We consider the process of ensemble formation (ensembling) as a means to distinguish the sources of generalization error in classification problems and to mitigate the stochasticity-related error of the models. By the term *learning procedure* we refer to the entirety of the process of model initialization, data acquisition and preparation, and derivation of model parameters.

We claim that the expected error rate of simple models (i.e. models that are not ensembles) can be decomposed into the generalization error of the underlying learning procedure as such, which quantifies the procedure's inductive bias (Belkin et al., 2019), and the *variance-error*, which quantifies the expected underspecification-related error of its induced models. D'Amour et al. (2020) characterize an ML pipeline as underspecified if it can yield multiple distinct predictors with similar (in-distribution) test set performance. We demonstrate this for the single-class classification datasets CIFAR-10 and CIFAR-100 by approximating the above decomposition with geometric mean-based deep ensembles (Lakshminarayanan et al., 2017) and present results that suggest that the out-of-distribution accuracy improvement through ensembling can be estimated through its effects on test set performance.

In this paper we aim to help better understand the difference between the over- and under-parameterized learning regimes in which machine learning takes place and to explore the potential of ensembling to help us understand and overcome the high error rates that can occur at the boundary of these two learning regimes. The transition between the two regimes takes place when the model is just barely able to encode all training data. This is the case when the model capacity marginally suffices to almost perfectly fit the training data and when the model receives sufficient computational resources (e.g. training epochs) to do so. As it marks the point where the model starts to afford interpolating the training data, the name of this transition is *interpolation threshold*. At around that threshold, under certain conditions, models exhibit markedly reduced generalization performance com-

Rath-Manakidis, P., Hlynsson, H. and Wiskott, L.
Reduction of Variance-related Error through Ensembling: Deep Double Descent and Out-of-Distribution Generalization.
DOI: 10.5220/0010821300003122
In *Proceedings of the 11th International Conference on Pattern Recognition Applications and Methods (ICPRAM 2022)*, pages 31-40
ISBN: 978-989-758-549-4; ISSN: 2184-4313

pared to similar models that have either an increased or even a decreased effective capacity to learn input regularities. This error hike at the border of the learning regimes gives rise to the double descent (DD) in the generalization error curve. In the case of deep neural networks (cf. Nakkiran et al., 2019) DD can be elicited in the absence of regularization through sufficiently strong label noise. We choose to approach this phenomenon using ensemble construction from the perspective of a tentative *error decomposition* in order to empirically approach the idea that any given stochastic learning procedure (and thus ML pipeline in general) can be seen as inducing a distribution over mappings (i.e. in the form of models) whose statistical properties can be studied.

2 RELATED WORK

Although first observed by Opper et al. (1990), explicit theoretic inquiry into DD started as late as 2018 with Belkin et al. (2019), who first coined the term. Belkin et al. (2019) have demonstrated model-wise DD in random Fourier Feature models, two layer neural networks and Random Forests. By initializing neural networks with small initial weights and by requiring minimum functional norm solutions for overspecified two-layer feature models they have demonstrated DD across models and datasets although they remained focused on models that are shallow by machine learning standards.

Most theoretical research around DD has up to now dealt with wide shallow one or two layer networks measuring network capacity based on layer widths (most notably Mei and Montanari, 2019; Advani et al., 2020; d'Ascoli et al., 2020). In most studies the first layer is random and fixed and weights are only learned for the linear second layer. Interpolation often occurs exactly at the point where the number of model parameters P equals the number of training samples N. A common feature of these works is that they deploy asymptotic analysis with P and N diverging to infinity and constant P/N by using random matrix theory to obtain expected values for the generalization error using randomly distributed artificial training data.

Deep DD refers to DD on highly non-linear networks with a large number of hidden layers. Up to now, there are, to our knowledge, no analytical techniques for demarcating the possible generality of this phenomenon. A promising direction is the study of Gaussian processes (Rasmussen, 2003) as they have been shown to behave like deep networks (Lee et al., 2017) in the limit of infinite layer width and to be mathematically well-characterized to the point that closed-form descriptions of the distribution of model predictions can be derived. A related promising field is kernel learning, because it is integral in the formal characterization of the aforementioned Gaussian processes w.r.t. their generalization error (Jacot et al., 2018) and because DD (see Belkin et al., 2018) occurs in this setting too.

Nakkiran et al. (2019) have demonstrated DD on image classification tasks using preactivation ResNet18 models and simpler stacked convolutional architectures on the CIFAR-10 and CIFAR-100 datasets. Yang et al. (2020) have expanded on the study of deep DD by decomposing the test loss into its bias and variance terms and have observed that under some settings the loss variance first monotonically increases until around the test error DD hike and monotonically decreases thereafter.

The paper by Geiger et al. (2020) is the work most closely related to this paper. The authors consider variance between classifiers derived from the same learning procedure. The learning scenarios they consider lack label noise and they attribute the variance to the variability in model parameter initialization. Among other setups, they consider linear and simple convolutional models on MNIST and CIFAR-10. They also conjecture that for over-parameterized networks the second descent is related to the weakening of fluctuations in the test error as the model is iterated. Geiger et al. (2020) also consider the trade-off between ensembling and using larger networks. We, on the other hand, consider scenarios with more realistic and larger neural networks where label noise is added to training data and deal with multiple dimensions of model complexity (training duration and model size) and compare the generalization performance of ensembles under distribution shift.

Adlam and Pennington (2020a) demonstrate in a realistic setting (and Chen et al. (2020) under more artificial conditions) that DD can be part of a more complicated test error curve resulting from an elaborate interplay between the specifics of the dataset structure and a learning procedure family's dispositions to capture it. Adlam and Pennington (2020a), in particular, find that a test error hike can appear when the number of parameters equals the training set size and, additionally, when it is equal to about the square of the number training data points. In another work Adlam and Pennington (2020b) also demonstrate that learning procedure variance can and should be decomposed further in order to make better sense of DD.

3 METHODS

The test error approximately quantifies the deficiency of a model's ability to capture the generalization distribution of the data. Yet, a learning procedure's deficiency need not be accurately reflected in the deficiency of any one particular model generated by it. Central tendencies of the distribution of the mappings of the models the learning procedure induces may capture the structure of the data better than any one particular model. The error of a stochastic learning procedure defined on some data distribution can therefore be thought of as the structure in the data which cannot be inferred using the procedure itself without additional knowledge about the problem domain, even when combining the outputs of infinitely many models. We choose ensembling as an approximation for the bias-variance decomposition of the test error for classification tasks. In particular, we find that the properties of geometric-mean based ensembling (following Yang et al., 2020) allow for a theoretically motivated combination of individual predictions that, in a meaningful and domain-agnostic way, utilize the degree of certainty of accepting or rejecting the different categorical outcomes of each predictor.

For a given x drawn from the generalization distribution and corresponding correct classification y and single-predictor output f the cross-entropy loss of learning procedure $\mathcal{T}$ decomposes as:

$$\mathop{\mathbb{E}}_{f\sim\mathcal{T}} H(y,f) = \underbrace{H(y)}_{\substack{\text{Irred.}\\ \text{Error}}} + \underbrace{D_{\mathrm{KL}}(y \,\|\, \bar{f})}_{\text{Bias}^2} + \underbrace{\mathop{\mathbb{E}}_{f\sim\mathcal{T}} D_{\mathrm{KL}}(\bar{f} \,\|\, f)}_{\text{Variance}} \tag{1}$$

where $\bar{f}$ is precisely the geometric mean-based mixture of estimators defined as:

$$\bar{f} \propto \exp\left[\mathop{\mathbb{E}}_{f\sim\mathcal{T}} \log f\right] \tag{2}$$

This mapping is approximated by the geometric-mean ensemble of i.i.d. models. By analogy, we consider the difference of the mean error rate of the constituent models and the error rate of the ensemble to be indicative of the distribution-specific underspecification of the ML pipeline realized by the learning procedure. This is a different quantity from the systematic error, which is manifested in the bias of the central tendency of the distribution of predictors.

The exact definition of the learning procedure under label noise depends on whether the introduction of noise is considered to be a part of the learning procedure. If it is, the approximation of the loss decomposition has to be carried out across sub-learners trained under i.i.d. noise-profiles each; alternatively, it has to be conducted using sets of sub-learners trained under fixed i.i.d. noise-profiles each. We propose a method (see Figure 1) for re-using one set of submodels for both configurations. In this way we reduce the overall number of models we need to train. Furthermore, by combining the same models in different ways the difference between the same-noise condition and the cross-noise condition is less affected by model variability and mainly results from the ensemble construction strategy. We combine the submodels for the cross-noise profile setting following the cyclical pattern depicted in Figure 1. We do so in order to minimize the effect of individual noise profiles on the average of measures over the ensembles. If we choose the number of distinct noise-profiles to be equal to the number of trials per noise-profile and sufficiently large, then we obtain an empirical fine-grained decomposition of the variance-error based on the different sources of randomness, i.e. data noise and model-derivation randomness.

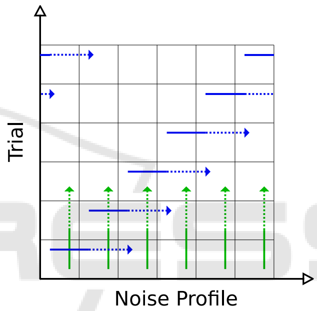

Figure 1: Configuration Design for Ensembling Strategy Comparison. Cross-noise profile ensembles are constructed following the horizontal arrows and same-noise profile ensembles following the vertical arrows.

The effective complexity of deep learning models depends on multiple parameters. Accordingly, we visualize the DD on the test error along the model width (model-wise DD) and the training epoch count (epoch-wise DD) in Figure 2. The model width is a factor in the number of convolutional channels used in the hidden layers of the VGG11 (Simonyan and Zisserman, 2014) and ResNet18 (He et al., 2016) visual classification models we consider in this paper. The ensembles considered in Figure 2 are cross-noise profile ensembles.

We compare different ensembling strategies and ensemble mixing functions as well as comparable non-ensemble architectures in order to be able to disentangle the effects of design components on generalization and on DD mitigation. We compare:

1. Single sub-learners trained with and without label noise.
2. Same-noise profile ensembles: Ensembles over models all trained under the same label noise pro-

file. We use the following mixing techniques for these ensembles:

(a) Learnable fully-connected bias-free linear ensembling with Softmax normalization. The outputs of the sub-learners are fed through a linear layer whose parameters are learned during an additional training process. This additional training is subject to the same noise profile that the sub-learners were subjected to.

(b) Arithmetic mean-based ensembling: The outputs for each category over all learners are mixed according to: $f_e = \frac{1}{N}\sum_{n=1}^{N} f_n$

(c) Geometric mean-based ensembling: The outputs for each category over all learners are mixed according to: $f_e \propto \sqrt[N]{\prod_{n=1}^{N} f_n}$

(d) Plurality vote-based ensembling: The category that is the first choice of the largest number of sub-learners is selected by the ensemble.

3. Cross-noise profile ensembles: Ensembles over models each trained under a different noise profile by using mixing techniques (b), (c) and (d).
4. *Mono-Ensembles*: Geometric mean-based ensemble architectures trained as single models under the same training configurations as the sub-learners.[1]
5. Large Networks: Networks of the same architecture type as the sub-learners, but with a parameter count as close as possible to multiples of the parameter count of the sub-learners and all training configurations left equal.

We are also interested in the implications of the underspecification-related performance penalty out-of-sample. To that end, we also study the effect of approximating the central tendency of learning procedures through ensembling on alternative datasets for the same classification problem. In particular, we test small ResNet18 classifiers that have been trained on CIFAR-10 that lie close to (width 12) or slightly beyond (width 26) the interpolation threshold on CIFAR-10.1 (Recht et al., 2018), CIFAR-10.2 (Lu et al., 2020), and the set of images contained in CINIC-10 (Darlow et al., 2018) that were adapted from ImageNet (Russakovsky et al., 2015). CIFAR-10.1 was designed to present almost no distribution shift w.r.t. standard CIFAR-10, whereas both CIFAR-10.2 and CINIC-10 were constructed to realize different data-distributions, e.g. regarding low level image statistics and the sub-categories (i.e. synonym sets) used for populating the classes.

Additional information on model training and experimental design along with further results is available in Rath-Manakidis (2021).

4 RESULTS

In this section we present the results of our experiments and describe their implications.

4.1 Findings on Double Descent

We observed no DD without noise on CIFAR-10. With almost no explicit regularization and without label noise, we obtained no epoch-wise DD on CIFAR-10 for neither ResNet18 nor VGG11 models. Therefore it is not possible in this case to empirically separate distinct learning regimes because the test error exhibits a global monotonous trend.

Under most configurations tested, we obtained epoch-wise DD w.r.t. the test set only w.r.t. the error and not the loss (see Plots 2b and 2c). This is surprising given the fact that it is the loss that the networks were trained to minimize and that it is merely intended as a proxy for the error that can be used in back-propagation[2], whereas in most other settings (e.g. in regression) the measure used in optimization itself exhibits DD on the test set. The test error is the metric we ultimately intend to minimize and the network is never confronted with it directly. For example, in Plot 2c we see that the loss does not display epoch-wise DD for this configuration and that it generally remains high, when compared to the values of its first descent. Nevertheless, the error performs a combined epoch-wise and model-wise DD. The loss does perform a weak model-wise DD for large epoch values but it does not reach again the values at the bottom of the first valley of its trajectory.

The valley in Plot 2b for the test error DD curve coincides with the valley of the noise-free train set error in 2a. This implies that the test error ascend is partly due to learning to fit label noise and is not a phenomenon tied strictly to generalization.

We find that ensembling of deep networks, especially if realized through a geometric mean-based approach to model output mixing, significantly improves model performance (see Figures 3 and 4). We attribute this to the capacity of the geometric-mean ensemble to differentiate between strong and weak preference for or against each category by the sub-models: if some models weakly favor one category

[1] During training, sub-network outputs passed on to the ensembling layer where saturated to be greater or equal to 10^{-5}. This prevents not-a-number errors.

[2] E.g. the loss criterion is such that even correctly classified training inputs keep contributing to the optimization signal to the network parameters.

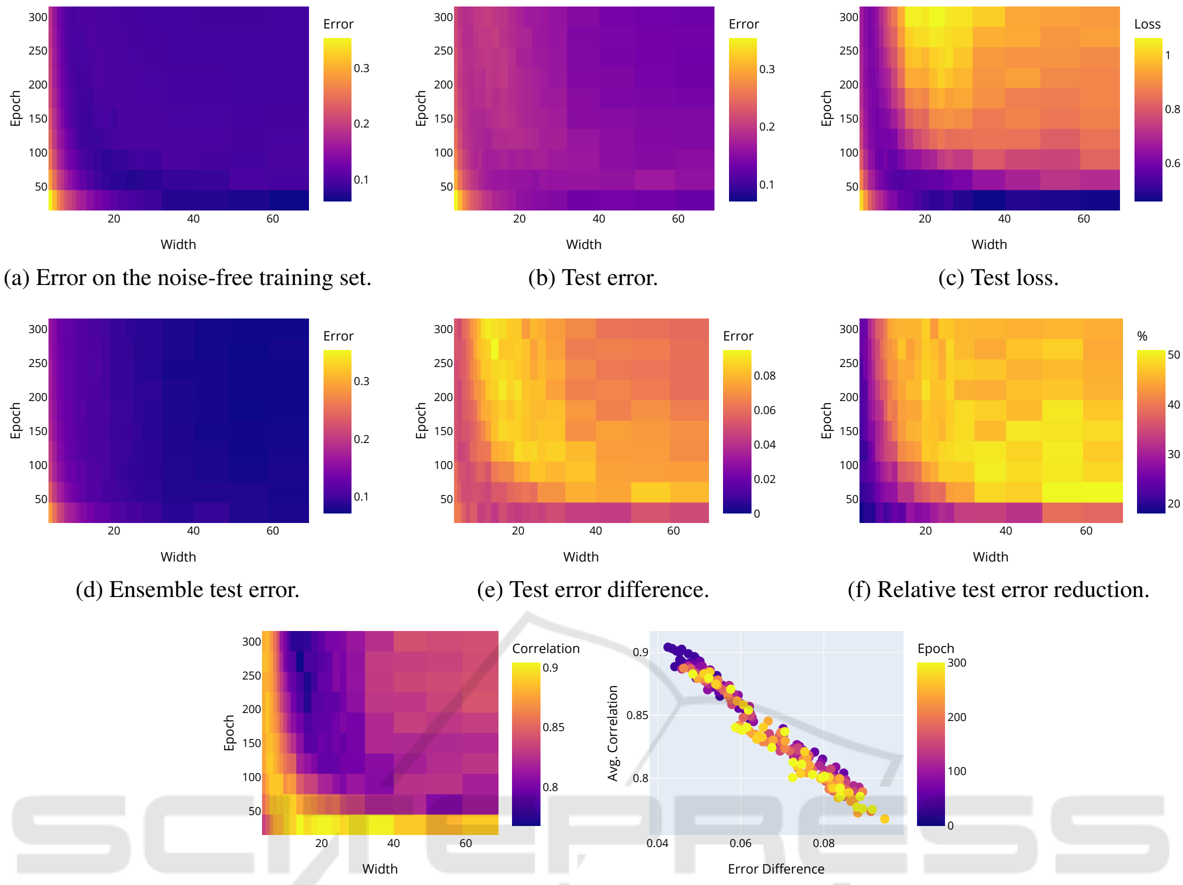

(a) Error on the noise-free training set.

(b) Test error.

(c) Test loss.

(d) Ensemble test error.

(e) Test error difference.

(f) Relative test error reduction.

(g) Output correlation.

(h) Accuracy increase against correlation.

Figure 2: Test error of ResNet18 on CIFAR-10. For each model-width and epoch combination we have rendered we ensemble 4 models with i.i.d. 10% label noise.

but a smaller number of models strongly prefer some other category, the latter option may still be preferred by the ensemble.

We find that those models that fall into the region of the interpolation threshold of the DD phenomenon profit most strongly from ensembling (see Plot 2e here and Figure 28 in Nakkiran et al., 2019). They do so in absolute and not in relative terms (cf. Plot 2f) in accordance with the interpretation that the benefits of ensembling hinge on the variability between the models. The observed performance improvement, at least for the case where it depends on the existence of label noise, can be realized by using same-noise profile ensembles almost as thoroughly as by cross-noise profile ensembles (see e.g. Figure 5). It also turns out that the generalization performance benefit of using cross-noise profile ensembles over same-noise profile ensembles tends to be statistically significant but quite small in magnitude. This means that around the DD hike most error variance of the learning procedure is accounted for by the network weight initialization and training-time randomness and only a small fraction of the variance can be additionally explained away in terms of the variation in the training noise profile. For ML deployment, this implies that artifacts in the training data that enter during data acquisition (i.e. that give rise to errors that constitute a noise profile) result, to a limited extend, in artifacts that cancel each other out in the learned function mappings.

We proceed to present some observations from the model type comparison in Figures 3 and 4. The geometric mean-based ensembler consistently outperforms all other ensembling methods, both with same-noise profile and cross-noise profile sub-learners for all ensemble sizes tested. We presume this is because geometric mean-based ensembling utilizes the available information better than the other two static approaches we tested: arithmetic mean-based ensembling fails to sufficiently reduce the impact of the votes of models that weakly prefer some output cat-

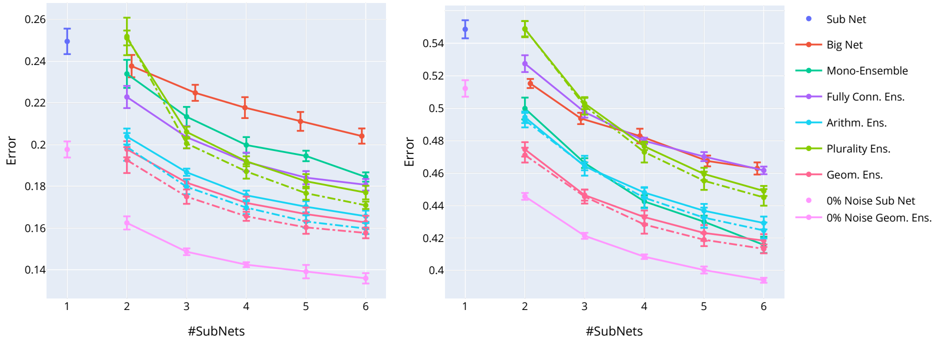

(a) CIFAR-10, sub-model width 9.

(b) CIFAR-100, sub-model width 11.

Figure 3: Test error of model trials based on VGG11. Continuous lines represent same-noise profile ensembles and dashed lines cross-noise profile ensembles. Noise strength is 10% for CIFAR-10 and 5% for CIFAR-100. The setups are explained in Section 3.

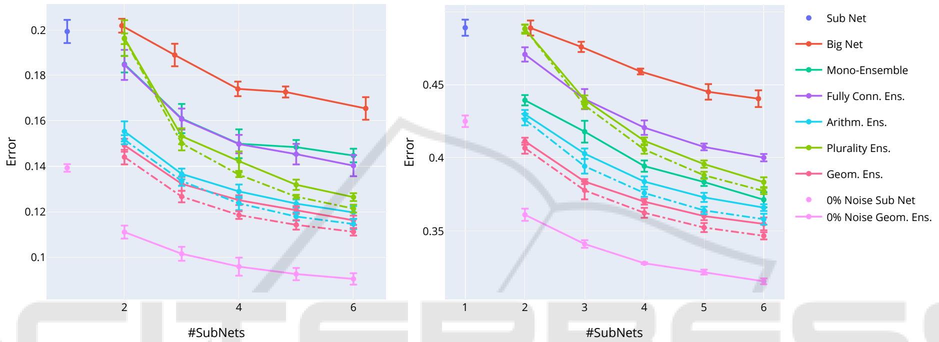

(a) CIFAR-10, sub-model width 10.

(b) CIFAR-100, sub-model width 11.

Figure 4: Test error of model trials based on ResNet18. Continuous lines represent same-noise profile ensembles and dashed lines cross-noise profile ensembles. Noise strength is 10%.

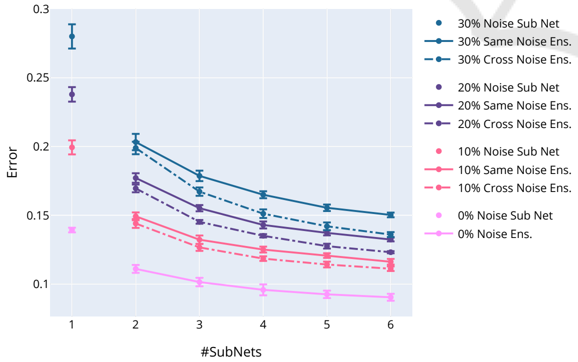

Figure 5: Test error of ResNet18 on CIFAR-10, model width 10. Continuous lines represent same-noise profile ensembles and dashed lines cross-noise profile ensembles. The colors code for noise strength.

egory over the others and plurality vote-based ensembling abstracts from any information regarding weak preference or strong rejection of categories. The additional training for the ensembles with a fully-connected linear layer as ensembling layer is less capable of facilitating generalization. The error backpropagation is conducted based on the error of the ensemble prediction rather than the errors of the predictions of the constituent modules for the mono-ensemble architecture. This architecture performs mostly worse than architecturally identical ensembles and better than monolithic architectures with equivalent parameter count.

With our experimental results we support the suggestion made by Geiger et al. (2020) that "..., given a computational envelope, the smallest generalization error is obtained using several networks of intermediate sizes, just beyond N^*, and averaging their outputs", under slightly more realistic conditions, whereby N^* refers to the interpolation threshold model parameterization. In Table 1 we show that a given computational envelope can be utilized more effectively if we train for a given type of model architecture many same-noise profile networks around the interpolation threshold in parallel and combine them for deployment, instead of training a large single network. In this way we require fewer computational steps for training and fewer parameters in total.

Table 1: Relative performance of ensembles and full-width networks for ResNet18 on CIFAR-10. The models were trained on 10% label noise and the ensembles are same-noise ensembles of 6 sub-learners. Models with widths 10 and 12 are interpolation threshold models. The mean performance of the ensembles of the models of width 10 and 12 is statistically significantly different from that of the full-width networks judging by the standard error of the mean.

Sub-model Width	#Parameters	Test Error Mean ± SEM
6	597696	0.1304 ± 0.00082
10	1649880	0.1162 ± 0.00084
12	2372100	0.1123 ± 0.00048
26	11088696	0.0919 ± 0.00058
Single net Width		
64	11173962	0.1307 ± 0.00180

4.2 Interpretation of Relative Model Performance

In those experiments where we have estimated the average performance of geometric mean-based ensembles, mono-ensembles and large networks (Figures 3 and 4), we see the general pattern that large networks perform worse than mono-ensembles which in turn tend to perform worse than geometric mean ensembles of the same-noise profile type.[3] We conjecture that this trend is due to internal correlations between the components (e.g. layers and channels) in some of the models. Table 1 shows that ensembles of models at the interpolation threshold can perform well while using relatively little memory. We attribute this to the good accuracy of their mean prediction and to the low degree of output correlation between these models (see Figures 2g and 2e) which permits extensive variance reduction through model averaging. We plot the accuracy increase due to ensembling against the strength of the correlations between the models constituting the ensemble in Plot 2h.

Geometric mean-based ensembles tend to perform better than comparable mono-ensembles (see e.g. Figure 3a). The latter differ from the former in that there is a shared last layer and that they are being trained through back-propagation on the loss of their *overall* predictions. Additionally, mono-ensembles face less diverse data shuffling and augmentation during training.[4]

Because of the two above-mentioned factors, during training there are identical influences on the sub-modules and the loss signal each sub-module is trained on is not specific to the individual module's divergence from the ground truth. This, in turn, may introduce correlations between the sub-modules, in the sense that it couples their training trajectories and causes the model as a whole to learn a less diverse and differentiated set of hidden features.

The worst performance in our comparison among models with an almost identical parameter count was that of large single networks. This can be attributed to the fact that the intermediary results of the computations in these models are used more often than in the other models. This leads to internal correlations between the parameters within the hidden layers of these models during back-propagation: In the large networks the number of parameters corresponding to each computational element (e.g. convolution channel) is larger than in the ensemble architectures and the internal state of the networks is more compact, i.e. fewer variables are used for storing intermediate results during forward-propagation. This impairs isolating relevant structure in the hidden features.

4.3 In-Distribution and Out-of-Distribution Generalization

For a given architecture, e.g. ResNet18 models of width 12 (Figure 6) or width 26 (Figure 7), the loss of the ensembles correlates linearly between different test sets as the number of sub-networks in the ensembles changes (cf. Miller et al., 2021). Likewise, a linear correlation also exists between the accuracy values on the different test sets. We also observe, as expected, that with increasing ensemble size the generalization performance increases and converges toward a limit. Simultaneously, the variance in the performance between distinct ensembles diminishes. We observe these trends for all transfer test sets we experimented on, regardless of the extend of distribution shift. This implies that the in-distribution benefit of ensembling predicts its out-of-distribution utility well. The increase in test-set performance by forming small ensembles can be used to estimate whether or not training further sub-models in order to form even larger ensembles is a worthwhile strategy for representing the meaningful structure of the problem at hand.

[3] With the exception of the experiment reported in Figure 3b where mono-ensembles outperform all regular ensembles.

[4] The input to each sub-module in the mono-ensemble for each training batch was always identical: it was not subject to independent selection and augmentation as was the case for the regular ensembles. This was necessary to reliably train all parameters using one loss signal.

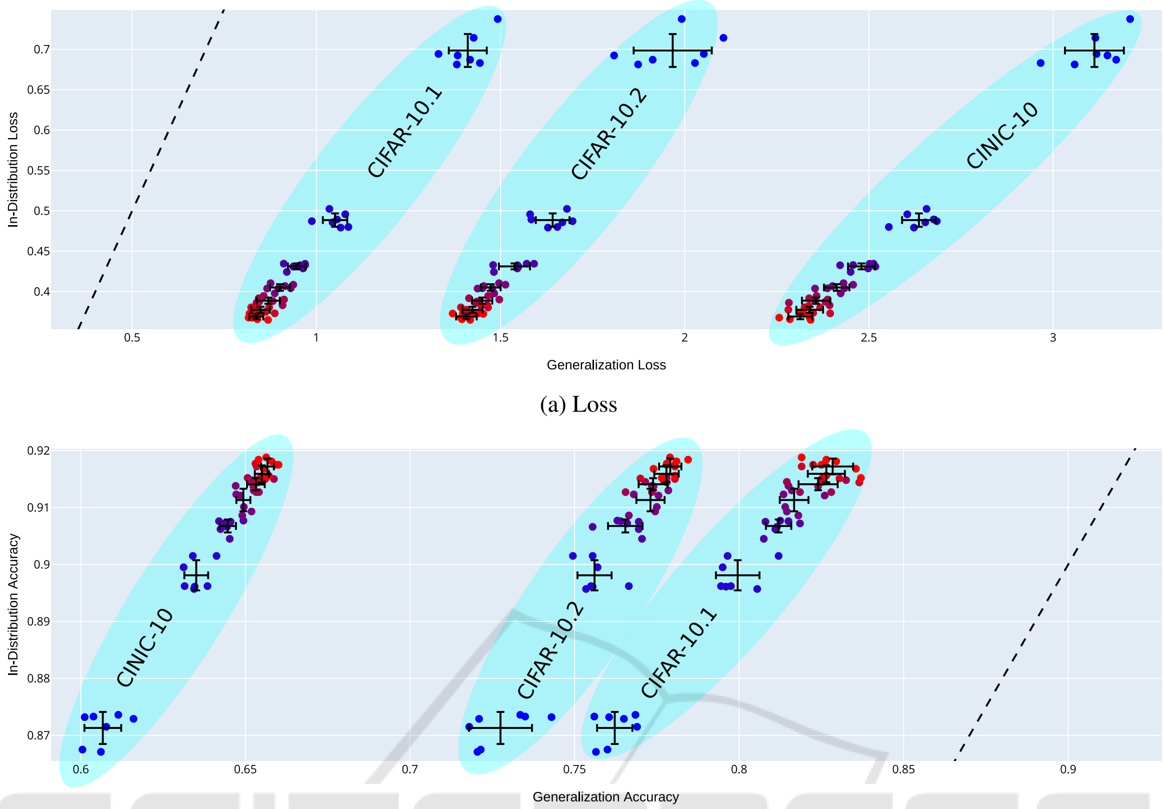

(a) Loss

(b) Accuracy

Figure 6: ResNet18 on CIFAR-10, model width 12. Blue points represent single models and red points ensembles of 7 models. Intermediary colors represent ensembles of sizes 2 to 6. We do not use label noise.

5 DISCUSSION

In this paper we present further examples of the DD generalization curve of the error on classification problems. Although we demonstrate a non-monotonous trend of the error for a range of up to now untested conditions and also approximate a bias-variance-decomposition of the error, the question in as far this is the same phenomenon that has been analysed in shallow models (e.g. Belkin et al., 2019; Advani et al., 2020; Mei and Montanari, 2019) remains open, because of the way loss and error relate and the fact that the trend of the error often contradicts that of its corresponding loss. This divergence is especially strong at and beyond the interpolation threshold and it raises the question in as far one could use alternative learning objectives to reliably mitigate the DD hike (cf. Ishida et al., 2020). We illustrate this divergence in Section 4.1 where we present results for deep learning settings for which certain types of DD occur only for the error and not for the loss.

In Table 1 we present the finding that small models that individually are impaired by DD can afford ensembles that outperform single large models while requiring considerably fewer overall parameters and computational steps. This has practical implications because it shows, that allowing for more intricate models with more complicated hidden features is not always the best approach to augment model performance if the model design suffers from underspecification. In particular, with a sufficiently general and reliable ensemble definition (geometric-mean ensembling) and with model and training procedure definitions that contain impactful sources of randomness we demonstrate how multiple predictors can be combined through ensembling to produce a considerably better model. This is the case even if we do not combine multiple learner types or strategies and without access to noise-free training data. The performance improvement through same-noise profile ensembling was on par with the improvement gained when also redrawing the noise on the training data (see Figure 5).

In Section 4.2 we propose an interpretation of the model architecture comparison in terms of coupled

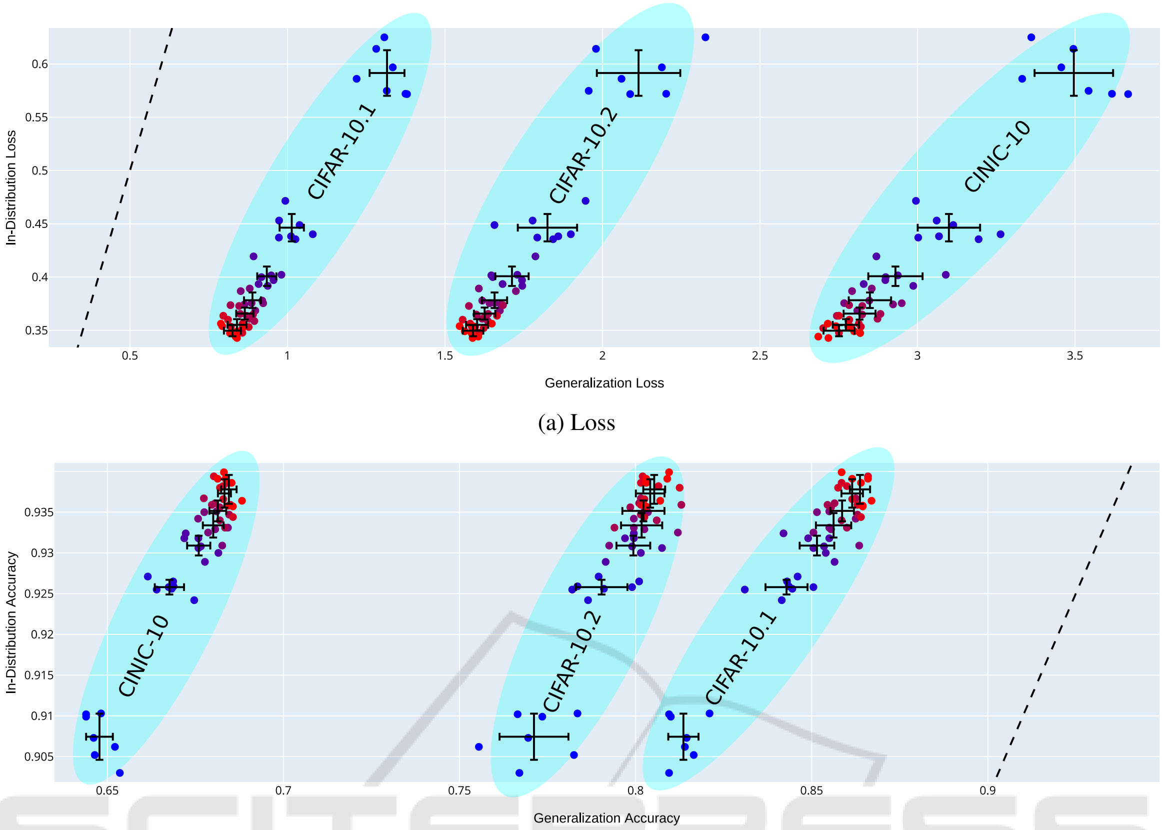

(a) Loss

(b) Accuracy

Figure 7: ResNet18 on CIFAR-10, model width 26. Same legend as for Figure 6.

training dynamics and ensuing model correlation that we hope will be scrutinized in future research. Future research is also needed to verify the degree of validity of the notion of error decomposition for classification problems and to mathematically ground the notion of a distribution of mappings and its evolution in the course of training.

With our out-of-distribution generalization experiments in Section 4.3 we show that the general trend of in-distribution generalization of increasingly large ensembles applies also to out-of-distribution settings and that the beneficial effects of ensembling generalize beyond the training distribution in a regular manner.

REFERENCES

Adlam, B. and Pennington, J. (2020a). The neural tangent kernel in high dimensions: Triple descent and a multi-scale theory of generalization. In *International Conference on Machine Learning*, pages 74–84. PMLR.

Adlam, B. and Pennington, J. (2020b). Understanding double descent requires a fine-grained bias-variance decomposition.

Advani, M. S., Saxe, A. M., and Sompolinsky, H. (2020). High-dimensional dynamics of generalization error in neural networks. *Neural Networks*, 132:428 – 446.

Belkin, M., Hsu, D., Ma, S., and Mandal, S. (2019). Reconciling modern machine-learning practice and the classical bias–variance trade-off. *Proceedings of the National Academy of Sciences*, 116(32):15849–15854.

Belkin, M., Ma, S., and Mandal, S. (2018). To understand deep learning we need to understand kernel learning. In *International Conference on Machine Learning*, pages 541–549. PMLR.

Chen, L., Min, Y., Belkin, M., and Karbasi, A. (2020). Multiple descent: Design your own generalization curve. *arXiv preprint arXiv:2008.01036*.

D'Amour, A., Heller, K., Moldovan, D., Adlam, B., Alipanahi, B., Beutel, A., Chen, C., Deaton, J., Eisenstein, J., Hoffman, M. D., Hormozdiari, F., Houlsby, N., Hou, S., Jerfel, G., Karthikesalingam, A., Lucic, M., Ma, Y., McLean, C., Mincu, D., Mitani, A., Montanari, A., Nado, Z., Natarajan, V., Nielson, C., Osborne, T. F., Raman, R., Ramasamy, K., Sayres, R., Schrouff, J., Seneviratne, M., Sequeira, S., Suresh, H., Veitch, V., Vladymyrov, M., Wang, X., Webster, K., Yadlowsky, S., Yun, T., Zhai, X., and Sculley, D. (2020). Underspecification presents challenges for credibility in modern machine learning. *arXiv preprint arXiv:2011.03395*.

Darlow, L. N., Crowley, E. J., Antoniou, A., and Storkey, A. J. (2018). CINIC-10 is not ImageNet or CIFAR-10. *arXiv preprint arXiv:1810.03505*.

d'Ascoli, S., Refinetti, M., Biroli, G., and Krzakala, F. (2020). Double trouble in double descent: Bias and variance (s) in the lazy regime. In *International Conference on Machine Learning*, pages 2280–2290. PMLR.

Geiger, M., Jacot, A., Spigler, S., Gabriel, F., Sagun, L., d'Ascoli, S., Biroli, G., Hongler, C., and Wyart, M. (2020). Scaling description of generalization with number of parameters in deep learning. *Journal of Statistical Mechanics: Theory and Experiment*, 2020(2):023401.

He, K., Zhang, X., Ren, S., and Sun, J. (2016). Deep residual learning for image recognition. In *Proceedings of the IEEE conference on computer vision and pattern recognition*, pages 770–778.

Ishida, T., Yamane, I., Sakai, T., Niu, G., and Sugiyama, M. (2020). Do we need zero training loss after achieving zero training error? In *International Conference on Machine Learning*, pages 4604–4614. PMLR.

Jacot, A., Gabriel, F., and Hongler, C. (2018). Neural tangent kernel: convergence and generalization in neural networks. In *Proceedings of the 32nd International Conference on Neural Information Processing Systems*, pages 8580–8589.

Lakshminarayanan, B., Pritzel, A., and Blundell, C. (2017). Simple and scalable predictive uncertainty estimation using deep ensembles. *Advances in Neural Information Processing Systems*, pages 6402–6413.

Lee, J., Bahri, Y., Novak, R., Schoenholz, S. S., Pennington, J., and Sohl-Dickstein, J. (2017). Deep neural networks as gaussian processes. *arXiv preprint arXiv:1711.00165*.

Lu, S., Nott, B., Olson, A., Todeschini, A., Vahabi, H., Carmon, Y., and Schmidt, L. (2020). Harder or different? a closer look at distribution shift in dataset reproduction. In *ICML Workshop on Uncertainty and Robustness in Deep Learning*.

Mei, S. and Montanari, A. (2019). The generalization error of random features regression: Precise asymptotics and double descent curve. *arXiv preprint arXiv:1908.05355*.

Miller, J. P., Taori, R., Raghunathan, A., Sagawa, S., Koh, P. W., Shankar, V., Liang, P., Carmon, Y., and Schmidt, L. (2021). Accuracy on the line: on the strong correlation between out-of-distribution and in-distribution generalization. In *International Conference on Machine Learning*, pages 7721–7735. PMLR.

Nakkiran, P., Kaplun, G., Bansal, Y., Yang, T., Barak, B., and Sutskever, I. (2019). Deep double descent: Where bigger models and more data hurt. *arXiv preprint arXiv:1912.02292*.

Opper, M., Kinzel, W., Kleinz, J., and Nehl, R. (1990). On the ability of the optimal perceptron to generalise. *Journal of Physics A: Mathematical and General*, 23(11):L581.

Rasmussen, C. E. (2003). Gaussian processes in machine learning. In *Summer school on machine learning*, pages 63–71. Springer.

Rath-Manakidis, P. (2021). Interaction of ensembling and double descent in deep neural networks. Master's thesis, Cognitive Science, Ruhr University Bochum, Germany.

Recht, B., Roelofs, R., Schmidt, L., and Shankar, V. (2018). Do CIFAR-10 classifiers generalize to CIFAR-10? *arXiv preprint arXiv:1806.00451*.

Russakovsky, O., Deng, J., Su, H., Krause, J., Satheesh, S., Ma, S., Huang, Z., Karpathy, A., Khosla, A., Bernstein, M., et al. (2015). Imagenet large scale visual recognition challenge. *International journal of computer vision*, 115(3):211–252.

Simonyan, K. and Zisserman, A. (2014). Very deep convolutional networks for large-scale image recognition. *arXiv preprint arXiv:1409.1556*.

Yang, Z., Yu, Y., You, C., Steinhardt, J., and Ma, Y. (2020). Rethinking bias-variance trade-off for generalization of neural networks. In *International Conference on Machine Learning*, pages 10767–10777. PMLR.